Relative Importance of the Operating Conditions Involved in the Formation of Nanoparticles of Ampicillin by Supercritical Antisolvent Precipitation

Alvaro Tenorio,* Maria D. Gordillo, Clara M. Pereyra, and Enrique J. Martínez de la Ossa

Department of Chemical Engineering, Food Technology and Environmental Technologies, Faculty of Sciences, University of Cádiz, 11510 Puerto Real (Cádiz), Spain

A screening design of experiments has been applied to the supercritical antisolvent precipitation of ampicillin (APC) using carbon dioxide (CO_2) and *N*-methylpyrrolidone (NMP) as antisolvent and solvent, respectively. The proposed design of experiment (DOE) is useful for identifying the key factors involved in the SAS process in just a few runs at an early stage of experimentation. Seven factors were studied, and two levels were assigned to each. A fractional factorial design with 2^{7-4} experiments plus two additional runs to calculate the accuracy of the estimates was used. The mean particle size (PS) and particle size distribution (PSD) of the processed ampicillin were chosen as responses to evaluate the process performance. Within the range of operating conditions investigated, concentration, temperature, and nozzle diameter proved to be the key factors having the greatest effect on both PS and PSD and, thus, the most important factors for controlling the formation of submicrometer particles of ampicillin by the SAS technique.

1. Introduction

Supercritical antisolvent (SAS) processes have been widely used to precipitate active pharmaceutical ingredients (APIs) for the past 10 years. These processes have, in most cases, yielded products with a high level of purity and suitable dimensional characteristics, such as particle sizes (PSs) in the micro- and nanometer ranges, narrow particle size distributions (PSDs), and spherical morphologies, for use in developing delivery systems for drug targeting and controlled release.[1−42]

Therefore, the SAS process is a promising micronization technique that is based on the particular properties of supercritical fluids (SCFs). These fluids have diffusivities that are 2 orders of magnitude larger than those of typical liquids, resulting in higher mass-transfer rates. The properties of SCFs (solvent power and selectivity) can be also adjusted continuously by altering the experimental conditions (temperature and pressure). As a consequence, the SCFs can be removed from the process by a simple change from supercritical to ambient conditions, which avoids difficult postprocess treatments of waste liquid streams. Of all possible SCFs, carbon dioxide (CO_2) at supercritical conditions is mainly used because of its relatively low critical temperature (31.1 °C) and pressure (73.8 bar), low toxicity, and low cost. Moreover, such supercritical conditions are sufficiently mild to permit the micronization of thermolabile solutes.

For all of these reasons, supercritical antisolvent techniques overcome the main drawbacks of conventional techniques, such as the degradation of the active ingredients because of the high profiles of temperatures and tensile stresses reached[43] and the large amount of organic solvent used, resulting in the need to remove the solvent from the final product. Moreover, conventional methods usually do not allow for very accurate control of the particle size, so that broad particle size distributions are obtained.

The supercritical antisolvent process uses both the high power of supercritical fluids to dissolve organic solvents and the low solubility of pharmaceutical compounds in supercritical fluids[35,44] to bring about the precipitation of these compounds when they are first dissolved in the organic phase and then brought into contact with the supercritical fluid. Therefore, the supercritical fluid has an antisolvent effect with respect of the solute to be micronized.

To carry out the supercritical antisolvent precipitation process, two operating modes are feasible. Batch processing, generally called gas antisolvent recrystallization (GAS), involves a full vessel of liquid solution being pressurized with carbon dioxide until supercritical conditions are reached. At that moment, the liquid phase is volumetrically expanded, causing the precipitation of the solute, which is then dried by passing pure SCF through the pressure vessel for an extended period (drying stage). In this operating mode, the rate of supercritical antisolvent addition can be an important parameter for controlling the morphology and size of the solid particles. The second mode is semicontinuous processing, which was developed with the aim of increasing the efficiency of the mass transfer between the two phases, so that the degree of control over the dimensional characteristics of the solid particles is improved, particularly in the micrometer and submicrometer ranges, and the drying stage is reduced.[45] These improvements are achieved basically by spraying an organic solution of API via a nozzle into the flowing stream of supercritical carbon dioxide. In this operating mode, the flow rates and their ratio can be important for the evolution of the precipitation process. Different names and acronyms have been used by various authors to describe this technique: supercritical antisolvent (SAS) process, aerosol solvent extraction system (ASES), and compressed antisolvent (PCA) process. A few studies have compared the GAS and SAS techniques, highlighting the improvements described above.[41,46]

A selection of APIs with particle sizes controlled by supercritical antisolvent techniques is shown in Table 1. Most of the research work was carried out considering the change of only one factor at a time, the others being held constant. The parameters whose effects have usually been investigated are the initial concentration of the solution (C), the temperature (T), the pressure (P), the solution flow rate (Q_L), and the carbon dioxide flow rate (Q_{CO_2}). However, the effects of other

* To whom correspondence should be addressed. Address: Department of Chemical Engineering, Food Technology and Environmental Technologies, Faculty of Sciences, University of Cádiz, 11510 Puerto Real (Cádiz), Spain. E-mail: alvaro.tenorio@uca.es. Tel.: + 34-956-016-458. Fax: + 34-956-016-411.

10.1021/ie0606441 CCC: $37.00
Published on Web 12/02/2006

Table 1. Effects of Operating Conditions on the Particle Size of APIs Processed by Supercritical Antisolvent Techniques[a]

active pharmaceutical ingredient (API)	operating conditions of supercritical antisolvent processes (GAS, SAS, ASES, SEDS)							
	C	T	P	Q_L	Q_{CO_2}	t_w	$Ø_n$	particle size range (μm)
tetracycline[4]	↔	–	↓	↔	↔	–	–	0.15−0.4
amoxicillin[5]	↑	↑	–	↔	↔	–	–	0.25−1.2
acetaminophen[8]	–	↑	↑	–	–	–	↑	3−20
nicotinic acid[9]	↑	↓	↑	–	↑	–	–	2−30
salbutamol[10]	↓	–	–	–	–	–	–	1−3
rifampicin[11]	↑	–	–	–	–	–	–	0.4−5
insulin[13]	↔	–	↔	↔	–	–	–	1−6.5
para-hydroxybenzoic acid[14]	↓	–	↓	↑	–	–	↓	3−6
sulfathiazole[20]	–	↔	–	–	↓	–	–	1−300
cefonicid[22]	↓	–	–	–	–	–	–	0.1−60
budesonide[26]	–	–	–	↔	↔	–	–	1.57−15.84
sulfarnethizole[28]	–	↑	–	–	↓	–	–	2−170
β-carotene[50]	↓	↑	↑	↓	↓	–	↑	1−2.3
amoxicillin[29]	↓	–	↑	–	–	–	–	0.1−1.2
salicylamide[32]	↓	↑	↓	↑	–	–	–	32−154.3
theophylline[33]	↓	–	↑	↔	–	–	–	15−500
BECD[35]	↓	↑	–	–	↓	–	–	1.8−43.9
atenolol[36]	–	–	–	↑	–	–	–	5−10
paracetamol[39]	↔	↑	–	–	↓	–	–	50−250
phenytoin[40]	–	–	–	–	↓	–	–	1−250
copper indometacin[41]	↓	↔	–	↔	–	–	↔	2−50

[a] Symbols: ↑, increase of the API mean particle size observed with an increase of the parameter; ↓, decrease of the API mean particle size observed with an increase of the parameter; ↔, negligible effect of the parameter on the API mean particle size observed; –, effect of the parameter was not examined.

parameters such as the washing time (t_w) and nozzle diameter ($Ø_n$) have not been widely examined. As can be seen in Table 1, contradictory results have been obtained by different authors with respect to the influence of the operating conditions on particle size: These results indicate how complex it is to establish rules of general behavior.

Therefore, in this article, we propose the design of experiments (DOE) as a suitable way to estimate the effects of all of the operating conditions involved in the SAS process (factors) on the selected product characteristics (responses) for the early stage of the investigation. In this way, for a certain system (API−solvent−supercritical CO_2), we will be able to identify the key factors of the SAS process with the aim of controlling the characteristics of the final product.

Ampicillin, one of the world's most widely prescribed antibiotics, is used to treat mainly infections of the middle ear, sinuses, bladder, and kidney, as well as uncomplicated gonorrhea. Using ampicillin microparticles of controlled size, it is possible to increase its bioavailability and decrease its therapeutic dosage (by improving efficiency). It is also possible to use various delivery system for the drug (transdermal, tracheobronchial, and pulmonary delivery systems).[16,47] Therefore, the mean particle size (PS) and particle size distribution (PSD) were selected as the specific responses for evaluating process performance.

With the aim of identifying the key variables or factors that control the formation of submicrometer particles of ampicillin by the SAS technique, and taking our previous experiments as the starting point, we applied a screening design of experiments (DOE) to the ampicillin (APC)−*N*-methylpyrrolidone (NMP) system. We considered seven factors (C, T, P, Q_L, Q_{CO_2}, t_w, and $Ø_n$) and two responses (PS and PSD) and evaluated each factor at two different levels.

2. Experimental Section

2.1. Materials and Analytical Methods. Ampicillin sodium salt (91.0% minimum purity) and 1-methyl-2-pyrrolidone (NMP) (99.5% purity) were purchased from Sigma−Aldrich Chemical (Madrid, Spain). Carbon dioxide with a minimum purity of 99.8% was supplied by Carburos Metálicos S.A. (Barcelona, Spain). The ampicillin was soluble in NMP for the fixed experimental concentration at room temperature. An SEM image of the as-received ampicillin is shown in Figure 1.

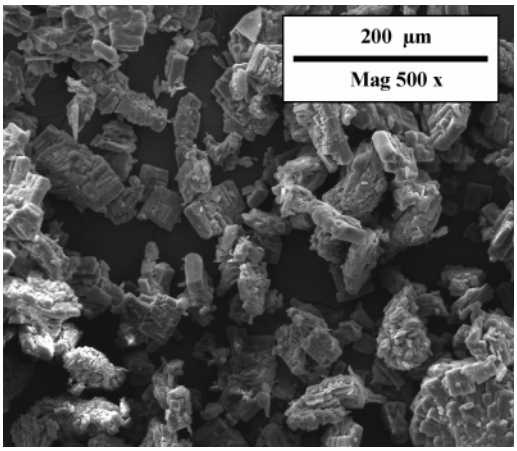

Figure 1. SEM image of unprocessed ampicillin.

Samples of the powder precipitated both on the wall and in the frit were observed using a SIRION FEG scanning electron microscope. Previously, the samples had been placed on carbon tape and then covered with a coating of gold using a sputter coater. The SEM images were processed using Scion image analysis software (Scion Corporation) to obtain the particle sizes. After that, the mean particle size (PS), standard deviation (SD) and coefficient of variation (CV), both as measurements of the distribution width, were calculated using Statgraphics plus 5.1 software. More than 800 particles were counted to perform the analysis in each experiment. X-ray diffraction pattern analysis (Bruker D8 Advance) was performed to determine the possible changes in the physical characteristics of the precipitate obtained by the SAS process.

2.2. Design of Experiments (DOE). In times past, the "one-factor-at-a-time" method has been a common route for investigating the effects of parameters on a process. By this method,

Table 2. Design Matrix, Responses, and Contrasts

run	C (1)	T (2)	P (3)	Q_L (4 = 123)	Q_{CO_2} (5 = 12)	t_w (6 = 23)	$Ø_n$ (7 = 13)	I	responses: mean PS (nm)	responses: coeff of variation	degree of success
20	+	+	−	−	+	−	−	+	−	−	0
29	−	−	+	+	+	−	−	+	−	−	0
39	−	+	+	−	−	+	−	+	99	0.286	1
42	+	−	−	+	−	+	−	+	291	0.406	1
70	+	−	+	−	−	−	+	+	395	0.368	1
75	−	+	−	+	−	−	+	+	−	−	0
113	−	−	−	−	+	+	+	+	−	−	0
128	+	+	+	+	+	+	+	+	224	0.389	1
					main effects of each variable on						
mean PS (nm)	204.3	**−181.5**	**−51.7**	10.5	**−37.7**	−	114.5	252.2			
coeff of variation	0.102	**−0.049**	**−0.058**	0.07	0.036	−	0.032	0.362			
degree of success						0.5					

the effects of one variable are calculated while all others are kept constant. However, it must be assumed that those effects will be the same even if the other variables are set at different levels, that is, that the effects of the variables are simply cumulative.

The DOE method is required not only to examine noncumulative effects but also to achieve higher accuracy. In particular by applying the factorial design at two levels, relevant trends for future experiments can be identified with only a few trials. In general, for K factors, the one-factor-at-a-time method would require K times more trials to be performed than the factorial design approach (2^K).

However, the number of trials required in a factorial design at two levels (2^K) increases with the number of factors K". As a consequence, the costs of resources needed to conduct experiments of a full factorial design can quickly become prohibitive. Fortunately, in most cases, when K is too high, the desired information can be obtained using only one fraction of the full factorial design. Nevertheless, this aspect must be taken into consideration.

A fractional factorial design is normally used for the early stages of an investigation where the study of the approximate influence of a large number of factors is more advisable than an accurate study of a few factors that could prove to be relatively unimportant.

In general, a fractional factorial design is created from the full factorial design at two levels. Some of the high-order interaction terms of the full factorial design are associated with additional experimental factors. Each pair of associated factors is called an alias, so the fractional factorial design is denoted as 2^{k-p}, where p is the number of aliases (pairs of allied factors).

In our study, we considered all factors that could have effects on the performance of the SAS process: the initial concentration of the solution, the temperature, the pressure, the liquid solution flow rate, the supercritical CO_2 flow rate, the washing time, and the nozzle diameter. The coding scheme used to describe the factor levels is based on the + and − signs, where + and − denote the high and low levels, respectively, of a factor.

From among all possible factorial fractional designs for seven factors at two levels, the design 2^{7-4} was selected because it allows the separation of the important effects from the unimportant effects with the smallest number of runs. The factorial fractional design 2^{7-4} has been successfully applied to several previous cases for screening purposes.[48,49]

In Table 2, the factorial design 2^{7-4} used in this work is shown; it was obtained as follows:

1. The full factorial design at two levels for concentration (1), temperature (2), and pressure (3) was built following the Yates standard order.[49]

2. Because there were four pairs of allied factors ($p = 4$), liquid flow rate (4), supercritical CO_2 flow rate (5), washing time (6), and nozzle diameter (7) were associated, respectively, with the following interactions: concentration/temperature/pressure (123), concentration/temperature (12), temperature/pressure (23), and concentration/pressure (13). The choice of allied factors was made considering that the factor that is thought to be the most likely to affect process performance is associated with the weaker interaction, in statistical terms. In general, interactions between three factors are less probable than interactions between two.[48] From the four factors liquid flow rate, CO_2 flow rate, washing time, and nozzle diameter, liquid flow rate was considered a priori to be the factor that has the major influence; hence, this factor was allied with the interaction of concentration/temperature/pressure (123). For this assumption, we took into account the fact that the inlet velocity of the solution was much higher than the inlet velocity of CO_2, so the liquid flow rate would have a greater relative influence on hydrodynamics and mixing of the process.[50] Thus, we expect the effect of the liquid flow rate to exclude any contribution of the concentration/temperature/pressure (123) interaction.

3. The signs of the new columns of allied factors were obtained by multiplying the signs of the variables that interact. For example, the signs of the concentration/temperature/pressure (123) column were obtained by multiplying the signs of the concentration column by the signs of the temperature column and by the signs of the pressure column.

As a result, eight different combinations of signs for the seven factors were generated, that is, eight different trials (20, 29, 39, 42, 70, 75, 113, and 128) out of the full factorial design at two levels 2^7. Thus, the design of Table 2 is a fraction of 1/16 of the full 2^7 design.

The next step was to understand what was included in each column. To determine the complete meaning of each column, a simple procedure involving the alias generators and contrast calculations was performed.[49] With the hypothesis that interactions between at least three factors are negligible, the set of aliases for each column could be simplified as shown in Table 3.

Therefore, the effect described in each column of Table 2 is due both to the effects of the main variables (C, T, P, Q_L, Q_{CO_2}, t_w, and $Ø_n$) and to the effects of the interactions shown in Table 3. For screening purposes, the interactions between two factors were also considered negligible, so the effect value l_i is caused

Table 3. Simplified Alias Structures

parameter	alias generator
concentration	$l_1 = 1 + 25 + 37 + 46$
temperature	$l_2 = 2 + 15 + 36 + 47$
pressure	$l_3 = 3 + 26 + 17 + 45$
liquid flow rate	$l_4 = 4 + 35 + 16 + 27$
supercritical CO_2 flow rate	$l_5 = 5 + 12 + 34 + 67$
washing time	$l_6 = 6 + 23 + 14 + 57$
nozzle diameter	$l_7 = 7 + 13 + 24 + 56$

Table 4. Two-Level Assessment for Each Factor

factor	low level	high level
C (mg/mL)	10	100
T (K)	308.15	328.15
P (bar)	90	180
Q_L (mL/min)	1	5
Q_{CO_2} (g/min)	32	66
t_w (min)	120	180
$Ø_n$ (m)	100	200

only by the main factor, i.e., concentration for column 1, temperature for column 2, and so on.

2.2.1. Level Identification. The two levels for each factor are shown in Table 4 and were chosen mainly on the basis of previous studies on SAS precipitation included in Table 1. However, various limiting conditions were set.

The low level of concentration was set to obtain a sufficient quantity of ampicillin for subsequent analysis, whereas the high level was limited by the saturation of the solution at room temperature.

The lower temperature limit was determined by the critical temperature of carbon dioxide, with the initial aim of staying within the supercritical domain; the upper limit was based on previous experience with the process, while also aiming at reducing energy costs. It was further considered that a range of 20 K would be sufficient to estimate the effect of temperature because such an increment leads to a large variation in the binary vapor−liquid equilibrium diagram of the NMP−CO_2 system[51] and thus in the results of the precipitation process.

The pressure condition limits were set with the aims of ensuring a high solubility of supercritical carbon dioxide in *N*-methylpyrrolidone (NMP) at two levels of temperature according to experimental data reported by Rajasingnam et al.[51] and of keeping the compression costs reasonable.

Flow rate limits were chosen to obtain both a wide range of NMP mass fraction within the precipitator vessel and a wide range of CO_2/NMP flow ratios, on the basis of previously performed studies.[4,5]

Regarding the washing times, the low level was selected considering that a minimum washing time is needed to avoid the recondensation of the liquid inside the chamber, which was estimated at 90 min,[4,5,10] whereas the high level was limited by energy costs. Finally, both the lower and upper nozzle diameters were limited by the design of our SAS apparatus.

2.2.2. Response Identification. Among the most important solid-state properties defined by the crystallization process are the dimensional properties of the final product (PS, PSD, and particle morphology) because these properties define some of the key characteristics of the product, such as processing behavior, particle permeability (API adsorption), and bioavailability (API absorption).[44]

Extensive research has shown that the critical aerodynamic diameter size of particles for aerosol delivery formulations is in the range of 1−5 μm.[4,14,16,44] In addition to being administered orally, nanoparticles (5−1000 nm) can also be delivered parenterally by intravenous, subcutaneous, and intraperitoneal means. Nanoparticles have a higher dissolution rate, a higher saturation solubility, and a greater adhesion than microparticles. Another major advantage of nanoparticles is that they are better at reaching the desired target organs than larger particles.[6,44]

Consequently, both the mean particle size (PS) and the particle size distribution (PSD) of the processed ampicillin were chosen as responses to evaluate the process performance.

However, because washing time acts once the particles are formed, to avoid the recondensation of the liquid inside the chamber, it is an essential stage for obtaining successful precipitation. Therefore, only the degree of success has been considered as the response with respect to the washing time factor. The degree of success is expressed numerically, as 0 when no powder was obtained and 1 for a successful precipitation, as indicated in Table 2.

2.3. Experimental Equipment and Procedures. A schematic diagram of the pilot plant, developed by Thar Technologies (model SAS 200), is shown in Figure 2. This equipment was used to carry out the experiments included in Table 2 plus two additional runs to calculate the accuracy of the estimates.

The SAS 200 system comprises the following components: two high-pressure pumps, one for the CO_2 (P1) and the other for the solution (P2), which incorporate a low-dead-volume head and check valves to provide efficient pumping of CO_2 and many solvents; a stainless steel precipitator vessel (V1) with a 2-L volume consisting of two parts, the main body and the frit, all surrounded by an electrical heating jacket (V1−HJ1); an automated back-pressure regulator (ABPR1) of high precision, attached to a motor controller with a position indicator; and a jacketed (CS1−HJ1) stainless steel cyclone separator (CS1) with 0.5-L volume, to separate the solvent and CO_2 once the pressure was released by the manual back-pressure regulator (MBPR1).

The following auxiliary elements were also necessary: a low-pressure heat exchanger (HE1), cooling lines, and a cooling bath (CWB1) to keep the CO_2 inlet pump cold and to chill the pump heads; an electric high-pressure heat exchanger (HE2) to preheat the CO_2 in the precipitator vessel to the required temperature quickly; safety devices (rupture discs and safety valve MV2); pressure gauges for measuring the pump outlet pressure (P1, PG1), the precipitator vessel pressure (V1, PG1), and the cyclone separator pressure (CS1, PG1); thermocouples placed inside (V1−TS2) and outside (V1−TS1) the precipitator vessel, inside the cyclone separator (CS1−TS1), and on the electric high-pressure heat exchanger to obtain continuous temperature measurements; and a FlexCOR coriolis mass flowmeter (FM1) to measure the CO_2 mass flow rate and another parameters such as total mass, density, temperature, volumetric flow rate, and total volume.

All factors that have an influence on the precipitation process (temperature, flow rate, pressure, etc.) could be controlled either manually or automatically (using ICM software).

A particularly important component of the SAS 200 system is the nozzle that sprays the liquid solution inside the precipitator vessel. Two commercial stainless steel nozzles from Thar Technologies with inner diameters of 100 and 200 μm were used in this work. Supercritical CO_2 was delivered from another inlet point located on the top of the vessel.

All experiments were performed following the same procedure. First, CO_2 was pumped into the vessel at the same time as the electrical heater, heat exchanger, and automatic back-pressure regulator were switched on. When CO_2 supercritical conditions (pressure and temperature) had been achieved and the solution pump had been primed, the liquid solution was pumped to the precipitator vessel and sprayed inside the vessel

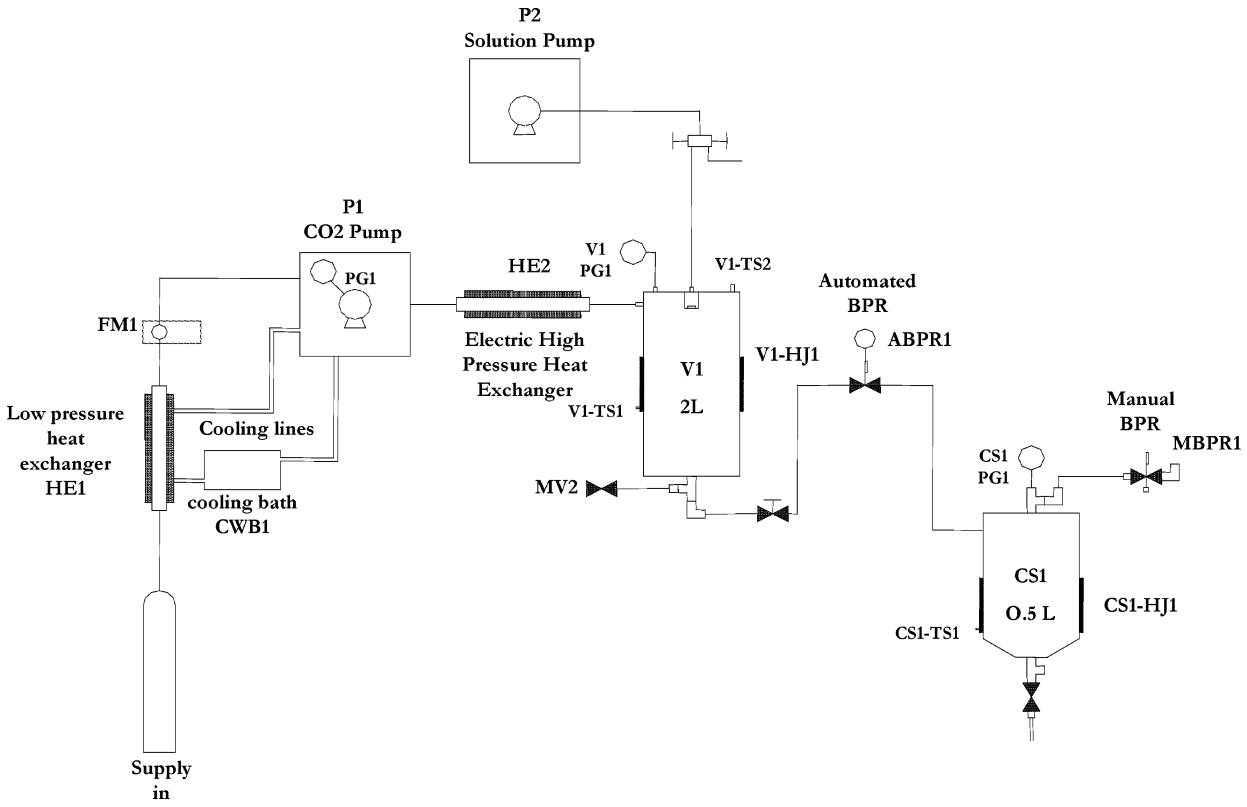

Figure 2. Schematic diagram of the pilot plant.

itself by means of the nozzle. The small drops of solvent were dissolved by the supercritical CO_2, causing supersaturation of the liquid solution and consequent precipitation of the ampicillin in the form of a powder that accumulated on the frit located at the bottom of the vessel; ampicillin powder also deposited on the internal wall of the vessel. The precipitation process ended when the desired amount of liquid solution had been fed into the system; then the liquid pump was turned off, and the supercritical CO_2 was allowed to continue flowing through the precipitator vessel to remove the residual content of the liquid solvent solubilized into the supercritical antisolvent (washing stage). After that, the supercritical CO_2 flow was stopped, and the system was depressurized to atmospheric pressure.

Finally, all of the precipitate was recovered from both the inner wall and the frit of the precipitator vessel; the analyses required, such as scanning electron microscope (SEM) and X-ray diffraction (XRD), were then carried out.

3. Results and Discussion

All experiments of the design matrix shown in Table 2 were carried out following the same experimental procedure, at the operating conditions indicated by the coding scheme (high and low levels of each factor).

Four of the eight experiments (39, 42, 70, and 128) included in the design matrix led to the successful precipitation of ampicillin. A considerable quantity of ampicillin precipitate both on the wall and in the frit of the precipitator vessel was obtained, particularly from experiments 39 and 128.

SEM images at the same magnification of ampicillin samples micronized in these experiments show the formation of spherical nanoparticles with a uniformly distributed mean particle size in the range of 99−395 nm and coefficients of variation within the range 0.286−0.406, as reported in Figure 3.

The ampicillin nanoparticle distribution can be fitted to log−normal distributions, which are compared in Figure 4, where the mean particle size (PS) and standard deviation (SD) are also shown. As can be seen in Figure 4, the smallest particle sizes with the narrowest particle size distribution were obtained from experiment 39, followed by those of the experiments 128, 42, and 70, respectively.

As discussed in Section 2.2, the effects reported in the columns of Table 2 are really composite values due to the effects of the main variables (C, T, P, $Q_{L,}$ Q_{CO_2}, t_w, and $Ø_n$) plus the effects of various interactions. However, for screening purposes, the interactions between two factors were considered negligible, so the effect value l_i can be taken as due only to the main factor. The term l_i can be calculated by means of eq 1, which represents the average response value for trials performed at the high level of the factor, minus the average response value for runs at the low level of the factor, i.e.

$$\text{effect } l_i = \frac{1}{N_+}\sum y_+ - \frac{1}{N_-}\sum y_- \qquad (1)$$

The trials without numerical values, such as 20, 29, 75, and 113, were discarded in the calculations of the main effect. As an example, the main effect of the concentration on particle size was calculated as

$$\text{effect } l_C = \frac{1}{3}(291 + 395 + 224) - \frac{1}{1}(99) = 204.3 \text{ nm}$$

Therefore, a change in the concentration from the low level to the high level means an increase of 204.3 nm in the particle size response.

The effects on the selected responses were calculated for each column and are reported at the bottom of Table 2. Moreover, with the aim of identifying the factors of major importance, an effect graph was plotted for both the particle size and particle size distribution (coefficient of variation) responses, as shown in Figure 5a and b, respectively.

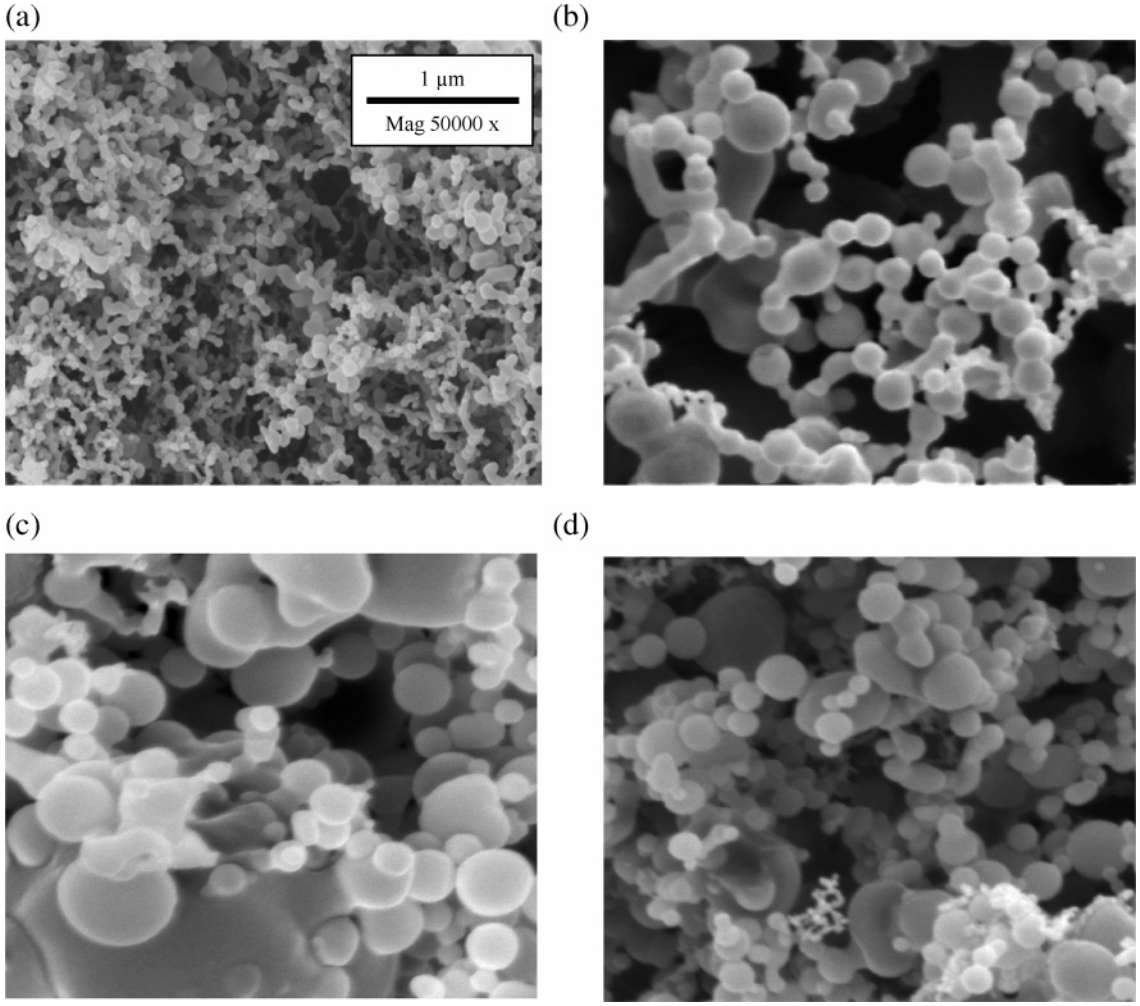

Figure 3. SEM image at the same enlargement of ampicillin nanoparticles precipitated from runs (a) 39, (b) 42, (c) 70, and (d) 128.

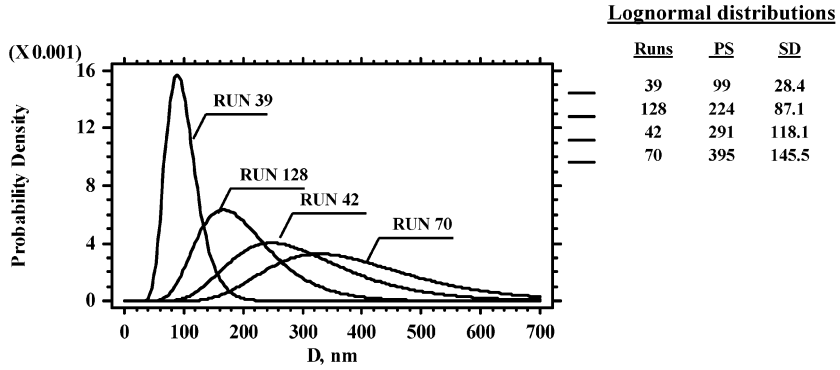

Figure 4. Probability density function of particle sizes for the experiments of the design matrix.

For the particle size response, the lowest slopes of the lines that connect the two average response values are for the liquid flow rate, the CO_2 flow rate, and the pressure. To assess whether such effects are significant, the variances of the effects were calculated according to the following equation[49]

$$V(\text{effect}) = \frac{4}{N}\sigma^2 \qquad (2)$$

To estimate the variance of elemental trials (σ^2), two additional runs of 70 were performed. An SEM image of ampicillin nanoparticles from one of the replicated runs of 70 is shown in Figure 6. Statistical calculations from the three runs of 70 show that the variance of the elemental trials is equal to 1584 and, using eq 2, the variance of the effect is equal to 792.

Therefore, the standard deviation of one effect is $\sqrt{792} \approx 28$, a value of approximately the same order of magnitude as the effects of the liquid flow rate, CO_2 flow rate, and pressure, which means that, within the range investigated, these factors have a negligible influence on the particle size.

On the other hand, three key factors with major effects on the particle size were identified. In order of decreasing importance, these are concentration, temperature, and nozzle diameter.

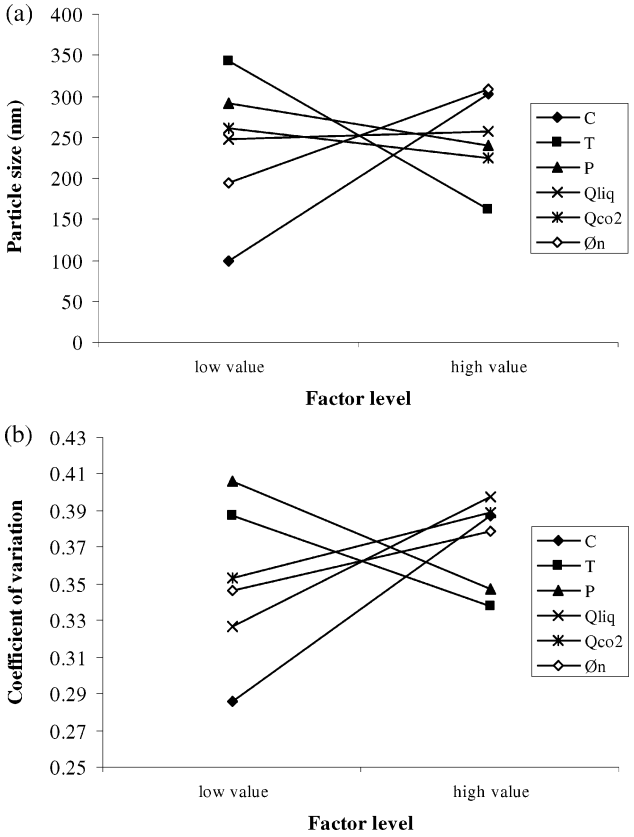

Figure 5. Main effect plots of the factors on (a) particles size and (b) particle size distribution.

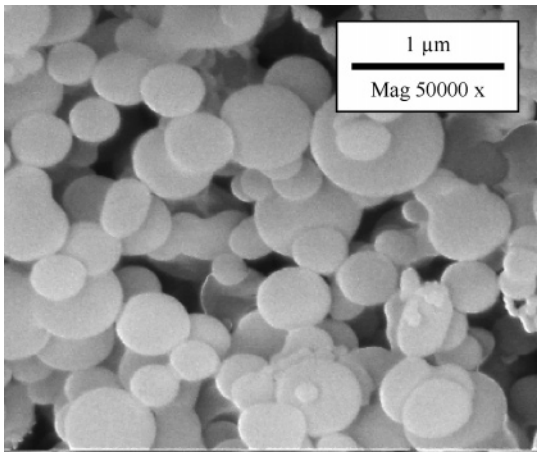

Figure 6. SEM image of ampicillin nanoparticles obtained from the replicated run 70.

The order of importance of the factors for particle size can be summarized as follows:

$$C > T, \varnothing_n > P, Q_{L,} Q_{CO_2}$$

A similar analysis was performed for the particle size distribution. From the relative slopes, it can be seen that the concentration factor has the major influence. The standard deviation of the effect estimated by the previous method is 0.006. Thus, none of the factors are hidden by experimental uncertainty so, within the investigated range, five key factors with a considerable influence were also identified. In order of decreasing importance, these are liquid flow rate, pressure, temperature, CO_2 flow rate, and nozzle diameter.

The order of importance of the factors for the particle size distribution can be summarized as follows:

$$C > Q_L, P, T > Q_{CO_2}, \varnothing_n$$

As shown in Figure 5a and b, an increase of the temperature leads to a decrease of both the PS and PSD. This finding can be explained on the basis of the numerical modeling of mass transfer proposed by Werling and Debenedetti.[52] According to experimental data reported by Rajasingnam et al.,[51] the CO_2−NMP system reaches miscible conditions (two phases are fully miscible) at the high level of pressure (180 bar) and at both levels of temperature studied (308 and 328 K). At miscible conditions, a higher mass-transfer rate is produced with increasing temperature at high pressure.[52] Thus, a higher degree of supersaturation is reached, resulting in a higher nucleation rate; a smaller PS and narrower PSD are thus obtained.

The tendency of particle size to vary with nozzle diameter is different: Nozzles of larger diameter produce larger particle sizes with broader distributions. At miscible conditions, distinct droplets are never formed, and the jet spreads, forming a gaseous plume, so that the system changes from an atomization process to a mixing process. Visual observations of the jet confirm this be true.[53,54] Thus, smaller nozzle diameters result in higher jet velocities, thus producing an increase in turbulence. The improvement of the mixing leads to higher supersaturations, and smaller particles are obtained.[50] Likewise, the degree of mixing can be modified with the liquid flow rate. In fact, this was taken to be an important factor in the design of experiments. However, within the range studied, the influence of the liquid flow rate on the degree of mixing, and thus on the particle size, was not noticeable. Similar experimental results were observed by other authors, as shown in Table 1.

As described above, the concentration is the factor that has the greatest influence on both the PS and the PSD. Therefore, both the PS and the PSD required for the final formulation of ampicillin could well be adjusted by a change in the initial concentration of the solution.

An increase in the initial concentration of the solution has two opposite effects: On one hand, with a higher concentration, it is possible to achieve higher supersaturations, which tend to diminish the particle size. On the other hand, condensation is directly proportional to the concentration of solute, and the increase of the condensation rate at higher concentrations tends to increase the particle size.[50]

In our case, an increase in the initial concentration of the solution led to larger particles sizes with a wider distribution. Thus, the second effect (condensation rate) prevailed under the operating conditions used in this work; that is, the higher the initial concentration of the solution, the higher the condensation rate, and thus, the greater the particle sizes produced. This result is consistent with those obtained by Reverchon et al.,[5] which were also explained in terms of competition between nucleation and growth processes.

Both pressure and CO_2 flow rate have substantial effects on the particle size distribution, but they exert their effects in different ways. If the flow rate of CO_2 is increased, a broad particle size distribution is obtained. On the other hand, an increase of pressure leads to a narrow particle size distribution. This fact can also be explained on the basis of the numerical modeling of mass transfer proposed by Werling and Debenedetti.[52] A pressure of 180 bar at both levels of temperatures studied brings the CO_2−NMP system to miscible conditions.[51] These conditions result in faster mass transfer, causing a higher

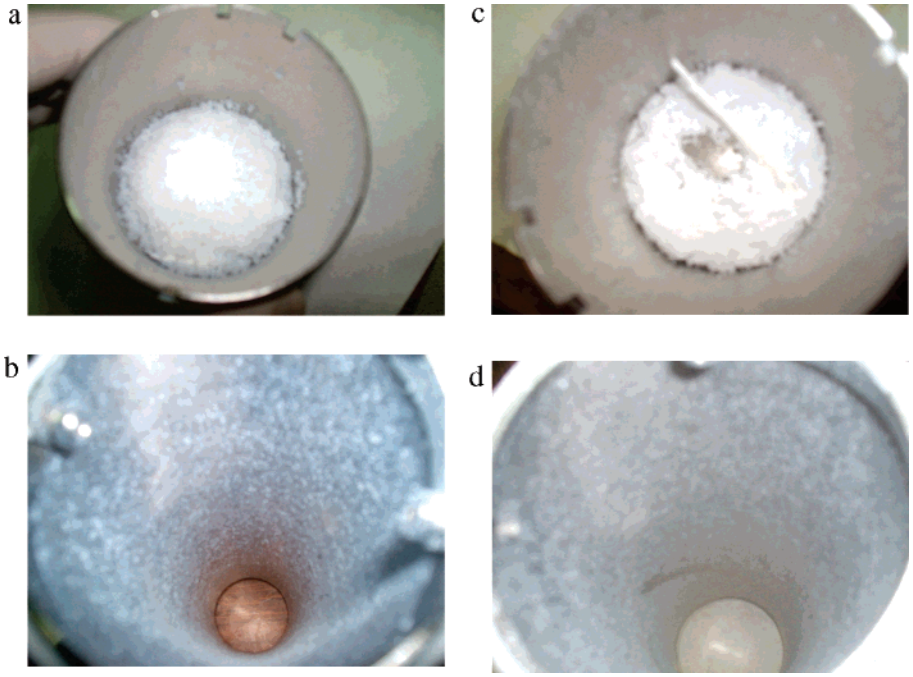

Figure 7. Images of ampicillin powders precipitated in the frit and on the wall of the precipitator vessel from runs (a,b) 39 and (c,d) 128.

degree of supersaturation that results in higher nucleation rates, thus producing a narrow particle size distribution.

As can be seen in Figure 7, the yield of the precipitation was particularly high in experiments 39 and 128, in which both temperature and pressure were set at their high levels. This finding confirms the importance of operating in the region of complete miscibility between NMP and CO_2.

Finally, the longer the washing time, the higher the degree of success (see Table 2). In other words, when the washing time was increased from 2 to 3 h, the probability of obtaining successful precipitation increased from 25% to 75%. Therefore, operation with the longer washing time is recommended.

Nevertheless, certain care must be taken when deep conclusions are drawn from this study. First, four trials of the design matrix (20, 29, 75, and 113) were not successful and generated no powder. Thus, the calculations of the main effects are more questionable from a statistical point of view. Moreover, to verify that the effect values l_i are due only to the main factor and not to the aliased interactions, a complementary set of experiments should be designed using the same design generators but with opposite signs. By this means, once the results of the two DOE sets are combined, all of the main factors would be free of interactions.

The possible structural changes of ampicillin suffered during the SAS process were evaluated by X-ray diffraction pattern analysis. XRD patterns of ampicillin nanoparticles and unprocessed ampicillin are shown in Figure 8. The ampicillin nanoparticles were found to have an amorphous structure. Such a change from crystalline to amorphous structure has been observed in a few other cases of precipitation of APIs by the SAS process and has been attributed to the very rapid precipitation that characterizes the SAS process, which does not allow time for the organization of the solute into a crystalline form.[4,5,11] Amorphous solids have a great ability to absorb water vapor into the bulk structure, forming an amorphous solution.[55] Therefore, the amorphous structure of ampicillin nanoparticles was also indicated by its rapid absorption of water vapor at a high level of relative humidity. The formation of an amorphous solution of ampicillin occurred suddenly at a relative humidity above approximately 60%. This high dissolution rate can be used to improve its therapeutic activity. However, formulations containing amorphous forms are less stable than their crystalline counterparts.[44,55]

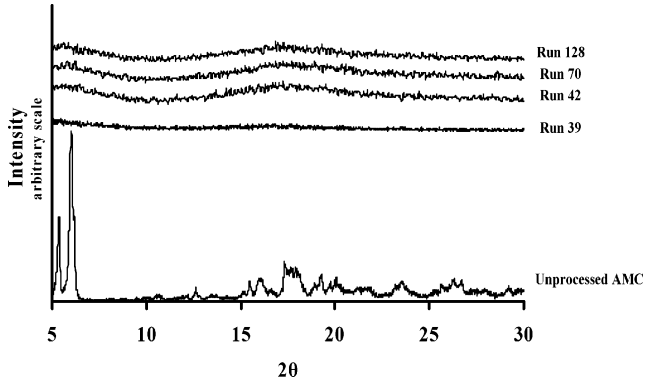

Figure 8. Comparison of ampicillin XRD patterns before and after SAS processing.

4. Conclusion

The supercritical antisolvent (SAS) process provides a feasible approach to the formation of ampicillin nanoparticles. Spherical ampicillin nanoparticles with a uniformly distributed mean particle size in the range of 99−395 nm were obtained from *N*-methylpyrrolidone (NMP).

The fractional factorial design 2^{7-4} was successfully applied to the APC−NMP system for screening purposes, allowing for the separation of the important effects from the unimportant effects in just a few runs. Three key factors with major effects on the particle size were identified. In order of decreasing importance, these are concentration, temperature, and nozzle diameter. A similar analysis was performed for the particle size distribution, identifying six key factors with a considerable influence. In order of decreasing importance, these are concentration, liquid flow rate, pressure, temperature, CO_2 flow rate, and nozzle diameter.

Among these important factors, the initial concentration of the solution is the factor that has the greatest influence on both the PS and the PSD. Therefore, it is the factor that allows better control in the formation of submicrometer particles of ampicillin by the SAS technique.

The yield of ampicillin precipitation was particularly high when the temperature and pressure were set at their high levels.

Therefore, to obtain the smallest particle sizes with the narrowest particle size distribution, an optimized selection of factor levels is proposed. From the results of the calculations of the main effects, the use of a low initial solution concentration and low liquid and CO_2 flow rates is advised. The diameter nozzle was found to be the factor that has the major influence on the hydrodynamics of the SAS process; therefore, it is convenient to use a smaller nozzle diameter to improve the degree of mixing and thus to obtain a higher degree of supersaturation. The optimized pressure and temperature are relatively high, with the object of staying in the region of complete miscibility between organic solvent and CO_2. Finally, operation with the long washing time is recommended.

Nevertheless, certain care must be taken when drawing deep conclusions from this study, because some trials were not successful, with no powder being obtained. Thus, the calculations of the main effects on the particle size and particle size distribution are less accurate from a statistical point of view.

The fractional factorial design used in this work is a helpful tool for establishing the effects of all operating conditions involved in the SAS process on the selected product characteristics. Thus, for a particular system (API−solvent−supercritical CO_2), we were able to identify the key factors of the SAS process for the control of the characteristics of the final product at an early stage of experimentation.

Acknowledgment

We gratefully acknowledge the INTERREG II-B program of the European Community and the Spanish Ministry of Science and Technology (Project PPQ2003-04245) for financial support.

Nomenclature

C = initial concentration of the solution, mg/mL
T = temperature of the precipitator vessel, K
P = pressure of the precipitator vessel, bar
Q_L = liquid flow rate, mL/min
Q_{CO_2} = supercritical CO_2 flow rate, g/min
t_w = washing time, min
$Ø_n$ = nozzle inner diameter, μm
l_i = main effects of each factor on the responses
y_+ = response value for trials performed at the high level of the factor
y_- = response value for trials performed at the low level of the factor
N_+ = total number of trials at the high level of the factor
N_- = total number of trials at the low level of the factor
N = number of elemental trials in the factorial design
σ^2 = variance estimated for the elemental trials

Literature Cited

(1) Chattopadhyay, P.; Gupta, R. B. Production of griseofulvin nanoparticles using supercritical CO_2 antisolvent with enhanced mass transfer. *Int. J. Pharm.* **2001**, *228*, 19−31.

(2) Steckel, H.; Thies, J.; Muller, B. W. Micronizing of steroids for pulmonary delivery by supercritical carbon dioxide. *Int. J. Pharm.* **1997**, *152*, 99−110.

(3) Steckel, H.; Muller, B. W. Metered-dose inhaler formulation of fluticasone-17-propionate micronized with supercritical carbon dioxide using the alternative propellant HFA-227. *Int. J. Pharm.* ***1998***, *173*, 25−33.

(4) Reverchon, E.; Della Porta, G. Production of antibiotic micro- and nano-particles by supercritical antisolvent precipitation. *Powder Technol.* ***1999***, *106*, 23−29.

(5) Reverchon, E.; Della Porta, G.; Falivene, M. G. Process parameters and morphology in amoxicillin micro and submicro particle generation by supercritical antisolvent precipitation. *J. Supercrit. Fluids* **2000**, *17*, 239−248.

(6) Chattopadhyay, P.; Gupta, R. B. Production of antibiotic nanoparticles using supercritical CO_2 as antisolvent with enhanced mass transfer. *Ind. Eng. Chem. Res.* ***2001***, *40*, 3530−3539.

(7) Moshashaee, S.; Bisrat, M.; Forbes, R. T.; Nyqvist, H.; York, P. Supercritical fluid processing of proteins I: Lysozyme precipitation from organic solution. *J. Pharm. Sci.* **2000**, *11*, 239−245.

(8) Bristow, S.; Shekunov, T.; Shekunov, B. Y.; York, P. Analysis of the supersaturation and precipitation process with supercritical CO_2. *J. Supercrit. Fluids* **2001**, *21*, 257−271.

(9) Rehman, M.; Shekunov, B. Y.; York, P.; Colthorpe, P. Solubility and precipitation of nicotinic acid in supercritical carbon dioxide. *J. Pharm. Sci.* ***2001***, *90*, 1570−1582.

(10) Reverchon, E.; Della Porta, G.; Pallado, P. Supercritical antisolvent precipitation of salbutamol microparticles. *Powder Technol.* ***2001***, *114*, 17−22.

(11) Reverchon, E.; De Marco, I.; Della Porta, G. Rifampicin microparticles production by supercritical antisolvent precipitation. *Int. J. Pharm.* ***2002***, *243*, 83−91.

(12) Reverchon, E. Supercritical-assisted atomization to produce micro- and/or nanoparticles of controlled size and distribution. *Ind. Eng. Chem. Res.* ***2002***, *41*, 2405−2411.

(13) Snavely, W. K.; Subramaniam, B.; Rajewski, R. A.; Defelippis, M. R. Micronization of insulin from halogenated alcohol solution using supercritical carbon dioxide as an antisolvent. *J. Pharm. Sci.* ***2002***, *91*, 2026−2039.

(14) Tu, L. S.; Dehghani, F.; Foster, N. R. Micronisation and micro encapsulation of pharmaceuticals using a carbon dioxide antisolvent. *Powder Technol.* ***2002***, *126*, 134−149.

(15) Velaga, S. P.; Ghaderi, R.; Carlfors, J. Preparation and characterisation of hydrocortisone particles using a supercritical fluids extraction process. *Int. J. Pharm.* ***2002***, *231*, 155−166.

(16) Reverchon, E.; Della Porta, G.; Spada, A. Ampicillin micronization by supercritical assisted atomization. *J. Pharm. Pharmacol.* ***2003***, *55*, 1465−1471.

(17) Reverchon, E.; Della Porta, G. Micronization of antibiotics by supercritical assisted atomization. *J. Supercrit. Fluids* **2003**, *26*, 243−252.

(18) Reverchon, E.; Della Porta, G. Terbutaline microparticles suitable for aerosol delivery produced by supercritical assisted atomization. *Int. J. Pharm.* ***2003***, *258*, 1−9.

(19) Shekunov, B. Y.; York, P.; Bristow, S.; Chow, A. H. L.; Cranswick, L.; Grant, D. J. W. Formation of composite crystals by precipitation in supercritical CO_2. *Cryst. Growth Des.* ***2003***, *3*, 603−610.

(20) Yeo, S.-D.; Kim, M.-S.; Lee, J.-C. Recrystallization of sulfathiazole and chlorpropamide using the supercritical fluid antisolvent process. *J. Supercrit. Fluids* **2003**, *25*, 143−154.

(21) Rehman, M.; Shekunov, B. Y.; York, P.; Lechuga-Ballesteros, D.; Miller, D. P.; Tan, T.; Colthorpe, P. Optimisation of powders for pulmonary delivery using supercritical fluid technology. *Eur. J. Pharm. Biopharm.* ***2004***, *22*, 1−17.

(22) Reverchon, E.; De Marco, L. Supercritical antisolvent micronization of Cefonicid: thermodynamic interpretation of results. *J. Supercrit. Fluids* **2004**, *31*, 207−215.

(23) Reverchon, E.; Spada, A. Erythromycin micro-particles produced by supercritical fluid atomization. *Powder Technol.* ***2004***, *141*, 100−108.

(24) Schiavone, H.; Palakodaty, S.; Tzannis, S. T.; Clark, A.; York, P. Evaluation of SCF-engineered particle-based lactose blends in passive dry powder inhalers. *Int. J. Pharm.* ***2004***, *281*, 55−66.

(25) Steckel, H.; Wehle, S. A novel formulation technique for metered dose inhaler (MDI) suspensions. *Int. J. Pharm.* ***2004***, *284*, 75−82.

(26) Steckel, H.; Pichert, L.; Müller, B. W. Influence of process parameters in the ASES process on particle properties of budesonide for pulmonary delivery. *Eur. J. Pharm. Biopharm.* ***2004***, *57*, 507−512.

(27) Velaga, S. P.; Bergh, S.; Carlfors, J. Stability and aerodynamic behaviour of glucocorticoid particles prepared by a supercritical fluids process. *Eur. J. Pharm. Biopharm.* ***2004***, *21*, 501−509.

(28) Yeo, S. D.; Lee, J. C. Crystallization of sulfarnethizole using the supercritical and liquid antisolvent processes. *J. Supercrit. Fluids* **2004**, *30*, 315−323.

(29) Kalogiannis, C. G.; Panayiotou, C. G.; Pavlidou, E. Production of amoxicillin microparticles by supercritical antisolvent precipitation. *Ind. Eng. Chem. Res*. ***2005***, *44*, 9339−9346.

(30) Liu, X.; Li, Z.; Han, B.; Yuan, T. Supercritical antisolvent precipitation of microparticles of quercetin. *Chin. J. Chem. Eng*. ***2005***, *13*, 128−130.

(31) Lobo, J. M.; Schiavone, H.; Palakodaty, S.; Tzannis, S. T.; York, P.; Clark, A. SCF-engineered powders for delivery of budesonide from passive DPI devices. *J. Pharm. Sci*. ***2005***, *94*, 2276−2288.

(32) Su, C.-S.; Chen, Y.-P. Recrystallization of salicylamide using a batch supercritical antisolvent process. *Chem. Eng. Technol*. ***2005***, *28*, 1177−1181.

(33) Subra, P.; Vega-González, A.; Laudani, C.-G.; Reverchon, E. Precipitation and phase behavior of theophylline in solvent−supercritical CO_2 mixtures. *J. Supercrit. Fluids* **2005**, *35*, 95−105.

(34) Velaga, S. P.; Carlfors, J. Supercritical fluids processing of recombinant human growth hormone. *Drug Dev. Ind. Pharm*. ***2005***, *31*, 135−149.

(35) Bakhbakhi, Y.; Charpentier, P. A.; Rohani, S. Experimental study of the GAS process for producing microparticles of beclomethasone-17,-21-dipropionate suitable for pulmonary delivery. *Int. J. Pharm*. ***2006***, *309*, 71−80.

(36) Kikic, I.; Alessi, P.; Eva, F.; Moneghini, M.; Perissutti, B. Supercritical antisolvent precipitation of atenolol: The influence of the organic solvent and of the processing approach. *J. Supercrit. Fluids* **2006**, *38*, 434−441.

(37) Della Porta, G.; Reverchon, E.; De Vittori, C. Supercritical assisted atomization: A novel technology for microparticles preparation of an asthma-controlling drug. *AAPS PharmSciTech* **2005**, 6.

(38) Reverchon, E.; Della Porta, G.; Spada, A.; Antonacci, A. Griseofulvin micronization and dissolution rate improvement by supercritical assisted atomization. *J. Pharm. Pharmacol*. ***2004***, *56*, 1379−1387.

(39) Fusaro, F.; Mazzotti, M.; Muhrer, G. Gas antisolvent recrystallization of paracetamol from acetone using compressed carbon dioxide as antisolvent. *Cryst. Growth Des*. ***2004***, *4*, 881−889.

(40) Muhrer, G.; Meier, U.; Fusaro, F.; Albano, S.; Mazzotti, M. Use of compressed gas precipitation to enhance the dissolution behavior of a poorly water-soluble drug: Generation of drug microparticles and drug-polymer solid dispersions. *Int. J. Pharm*. ***2006***, *308*, 69−83.

(41) Warwick, B.; Dehghani, F.; Foster, N. R.; Biffin, J. R.; Regtop, H. L. Micronization of copper indomethacin using gas antisolvent processes. *Ind. Eng. Chem. Res*. ***2002***, *41*, 1993−2004.

(42) Mammucari, R.; Dehghani, F.; Foster, N. R. Dense gas processing of micron-sized drug formulations incorporating hydroxypropylated and methylated beta-cyclodextrin. *Pharm. Res.* **2006**, *23*, 429−437.

(43) Hixon, L.; Prior, M.; Prem, H.; Van Cleef, J. Sizing materials by crushing and grinding. *Chem. Eng. (New York)* **1990**, *97*, 94−103.

(44) Shekunov, B. Y.; York, P. Crystallization processes in pharmaceutical technology and drug delivery design. *J. Cryst. Growth* **2000**, *211*, 122−136.

(45) York, P. Strategies for particle design using supercritical fluid technologies. *Pharm. Sci. Technol. Today* **1999**, *2*, 430−440.

(46) Fusaro, F.; Haenchen, M.; Mazzotti, M.; Muhrer, G.; Subramaniam, B. Dense Gas Antisolvent Precipitation: A Comparative Investigation of the GAS and PCA Techniques. *Ind. Eng. Chem. Res*. ***2005***, *44*, 1502−1509.

(47) Wiedmann, T. S. Pharmaceutical Inhalation Aerosol Technology. *J. Controlled Release* **2005**, *105*, 177−178.

(48) Subra, P.; Jestin, P. Screening design of experiment (DOE) applied to supercritical antisolvent process. *Ind. Eng. Chem. Res*. ***2000***, *39*, 4178−4184.

(49) Box, G. E. P.; Hunter, W. G.; Hunter, J. S. *Statistics for Experimenters. An Introduction to Design, Data Analysis and Model Building*; J. Wiley and Sons: New York, 1993.

(50) Martin, A.; Cocero, M. J. Numerical modeling of jet hydrodynamics, mass transfer, and crystallization kinetics in the supercritical antisolvent (SAS) process. *J. Supercrit. Fluids* **2004**, *32*, 203−219.

(51) Rajasingam, R.; Lioe, L.; Pham, Q. T.; Lucien, F. P. Solubility of carbon dioxide in dimethylsulfoxide and N-methyl-2-pyrrolidone at elevated pressure. *J. Supercrit. Fluids* **2004**, *31*, 227−234.

(52) Werling, J. O.; Debenedetti, P. G. Numerical modeling of mass transfer in the supercritical antisolvent process: Miscible conditions. *J. Supercrit. Fluids* **2000**, *18*, 11−24.

(53) Kerst, A. W.; Judat, B.; Schlunder, E.-U. Flow regimes of free jets and falling films at high ambient pressure. *Chem. Eng. Sci*. ***2000***, *55*, 4189−4208.

(54) Chehroudi, B.; Cohn, R.; Talley, D. Cryogenic shear layers: experiments and phenomenological modeling of the initial growth rate under subcritical and supercritical conditions. *Int. J. Heat Fluid Flow* **2002**, *23*, 554−563.

(55) Evgenyi Y. Shalaev, G. Z. How does residual water affect the solid-state degradation of drugs in the amorphous state? *J. Pharm. Sci*. ***1996***, *85*, 1137−1141.

Received for review May 23, 2006
Revised manuscript received September 8, 2006
Accepted October 24, 2006

IE0606441